



Supplementary Materials

A Comparative Study of the Influence of Nitrogen Content and Structural Characteristics of NiS/Nitrogen-Doped Carbon Nanocomposites on Capacitive Performances in Alkaline Medium

Mohamed M. Abdelaal ^{1,2,†}, Tzu-Cheng Hung ^{1,†}, Saad Gomaa Mohamed ², Chun-Chen Yang ^{1,3,4}, Huei-Ping Huang ¹ and Tai-Feng Hung ^{1,*}

¹ Battery Research Center of Green Energy, Ming Chi University of Technology, 84 Gungjuan Rd., Taishan District, New Taipei City 24301, Taiwan; mohamedbec@yahoo.com (M.M.A.); u07137023@mail2.mcut.edu.tw (T.-C.H.); ccyang@mail.mcut.edu.tw (C.-C.Y.); cindy118036@mail.mcut.edu.tw (H.-P.H.)

² Tabbin Institute for Metallurgical Studies (TIMS), Tabbin, Helwan 109, Cairo 11421, Egypt; sgmmohamed@gmail.com

³ Department of Chemical Engineering, Ming Chi University of Technology, 84 Gungjuan Rd., Taishan District, New Taipei City 24301, Taiwan

⁴ Department of Chemical and Materials Engineering, Chang Gung University, 259 Wenhua 1st Rd., Guishan District, Taoyuan 33302, Taiwan

* Correspondence: taifeng@mail.mcut.edu.tw; Tel.: +886-2-2908-9899 (ext. 4957)

† These authors contributed to this work equally.

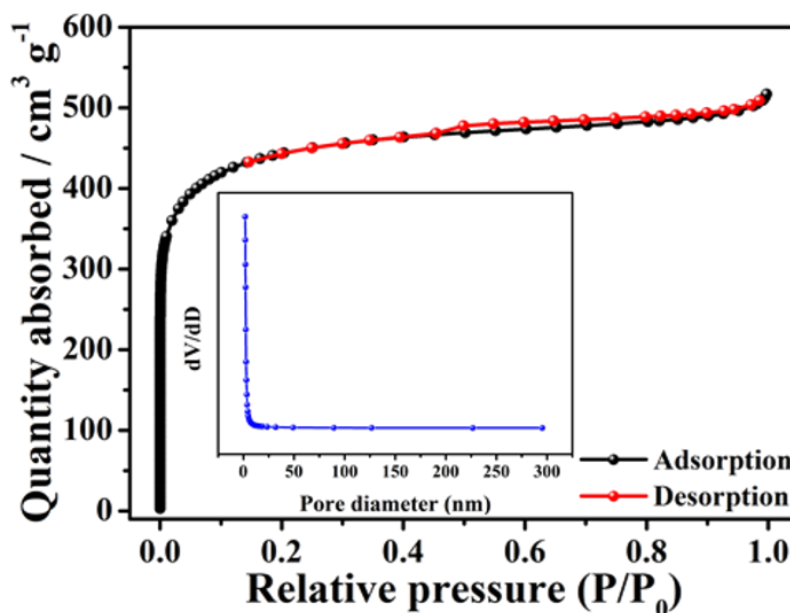
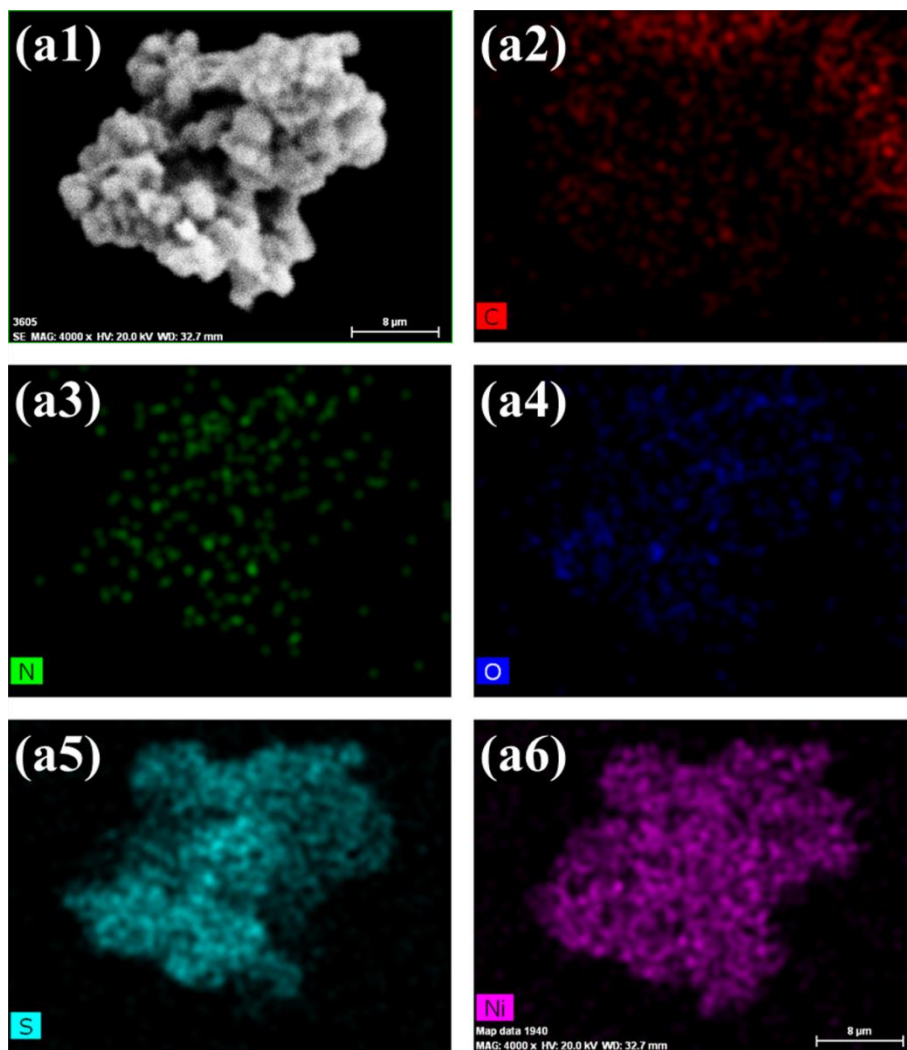


Figure S1. Nitrogen adsorption-desorption isotherm of A-PVP-NC collected by an accelerated surface area and porosimetry system at 77 K. Inset shows the pore size distribution curve calculated by BJH model.



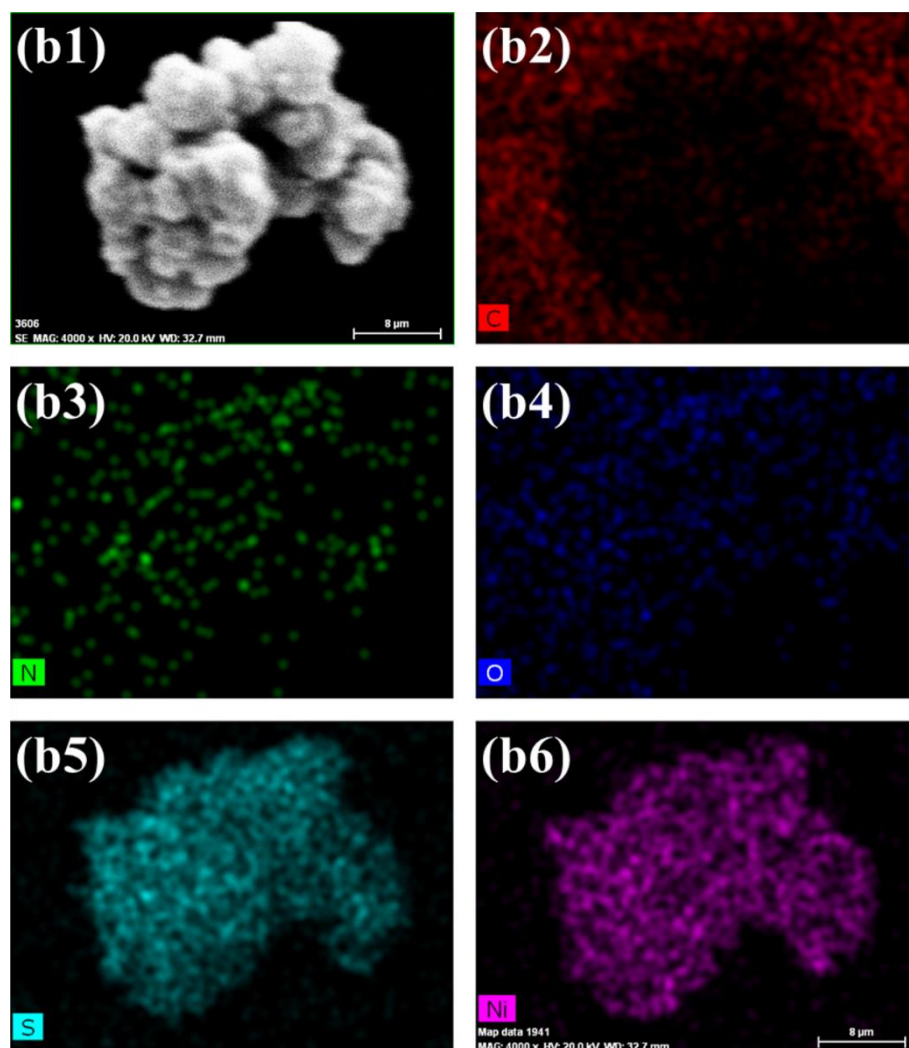


Figure S2. SEM-DEX mappings of (a) NiS-A-PVP-NC: (a1) SEM micrograph, (a2) carbon mapping, (a3) nitrogen mapping, (a4) oxygen mapping, (a5) sulfur mapping, (a6) nickel mapping and (b) NiS-PI-NC: (b1) SEM micrograph, (b2) carbon mapping, (b3) nitrogen mapping, (b4) oxygen mapping, (b5) sulfur mapping, (b6) nickel mapping. Scale bar: 8 μ m.

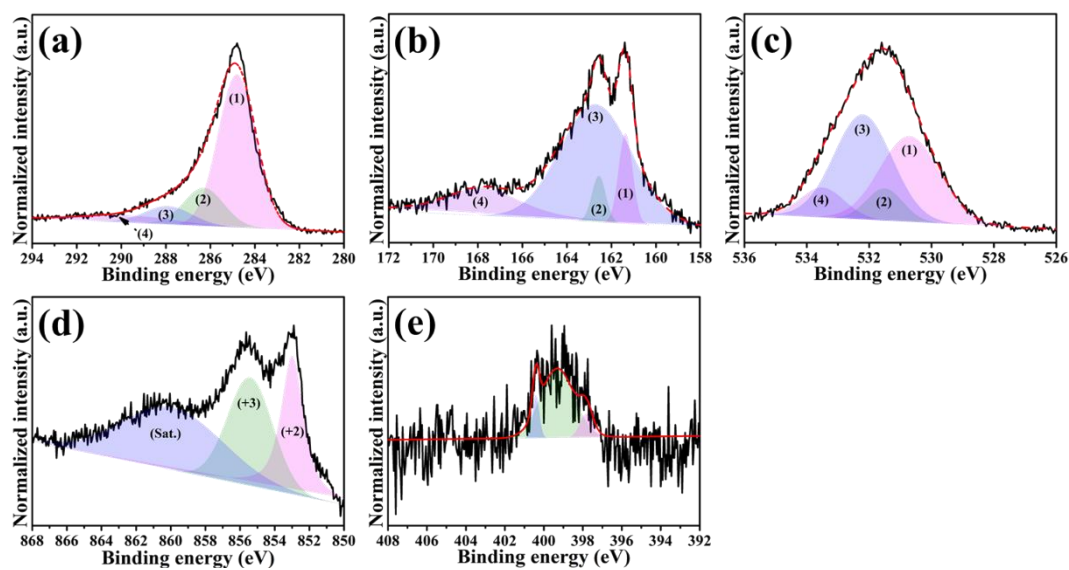


Figure S3. High-resolution XPS spectra of the NiS/A-PI-NC: (a) C 1s ((1) for C=C bond, (2) for C-O bond, (3) for C=O bond, and (4) for O=C-O bond), (b) S 2p ((1)-(3) assigned to S^{2-} within the NiS, and (4) from sulfate ions), (c) O 1s ((1) and (3) are associated with the $Ni^{3+}OOH$ and $Ni^{2+}SO_4$, (2) for O=C-O bond, and (4) for C=O bond), (d) Ni 2p and (e) N 1s.

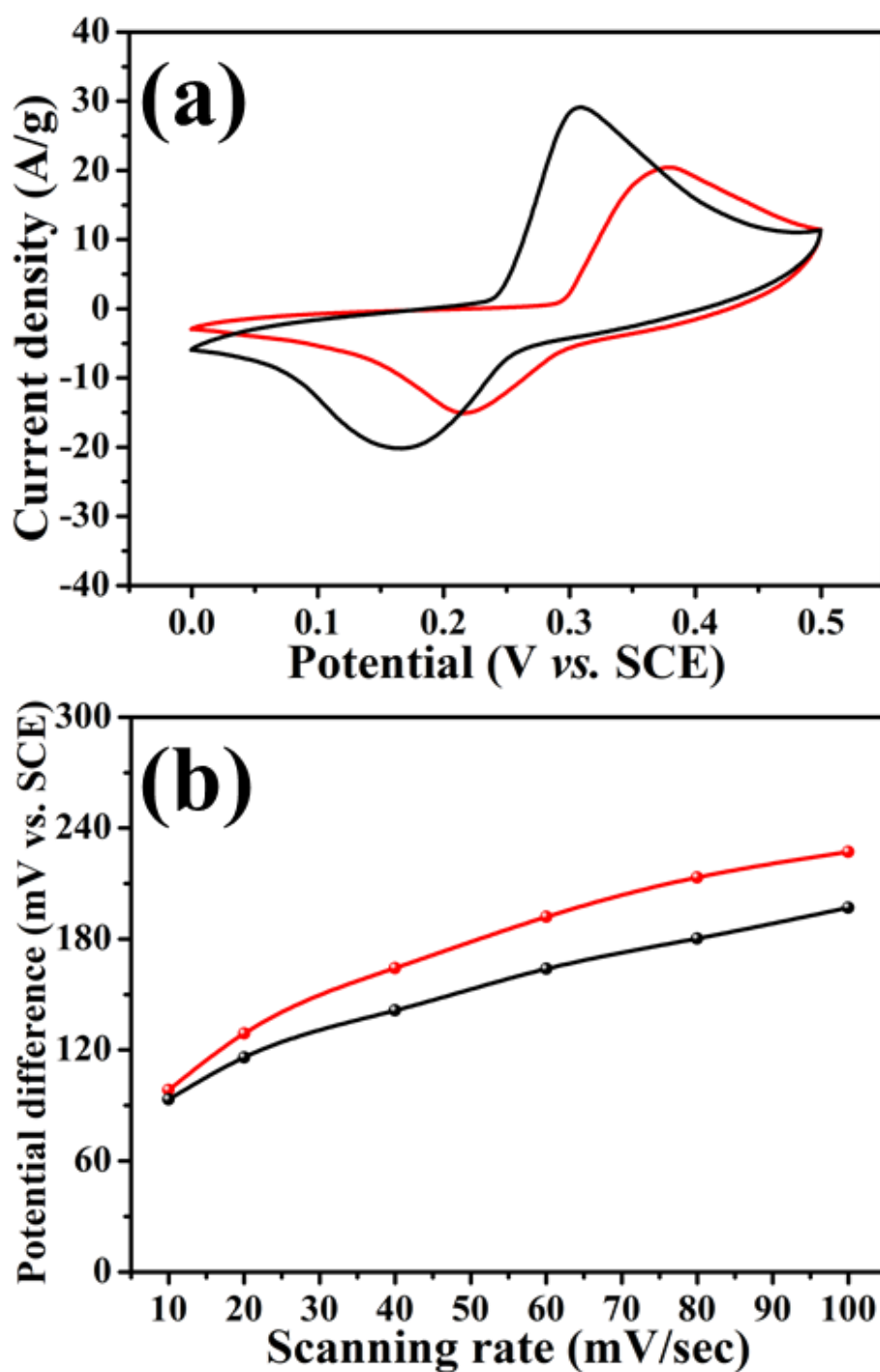


Figure S4. (a) Cyclic voltammograms of NiS/A-PVP-NC (-) and NiS/PI-NC (-), and (b) potential differences between anodic and cathodic peak positions of NiS/A-PVP-NC (•) and NiS/PI-NC (•).

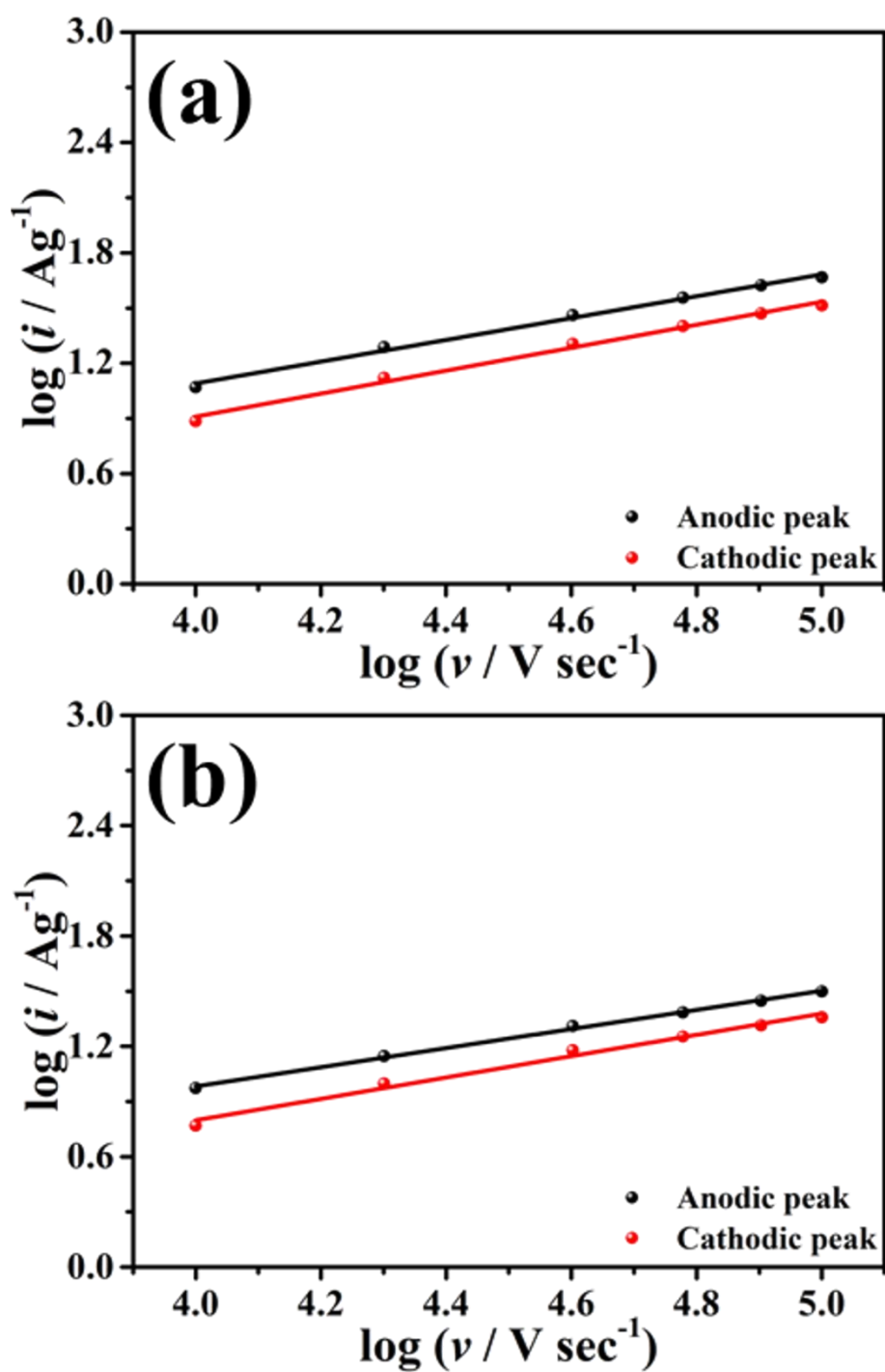


Figure S5. Anodic and cathodic current densities ($\log(i)$) of (a) NiS/A-PVP-NC and (b) NiS/PI-NC plotted as a function of scan rate ($\log(\nu)$).

Table S1. Textural properties of the A-PVP-NC.

Sample	SSA ¹ (m ² /g)	V _t ² (cm ³ /g)	V _{ultra} ³ (cm ³ /g)	V _{micro} ⁴ (cm ³ /g)	V _{meso} ⁵ (cm ³ /g)
A-PVP-NC	1628	0.79	0.25	0.62	0.17

¹SSA: Specific surface area calculated by the Brunauer-Emmett-Teller method.

²V_t: total pore (single-point) volume obtained from the amount of adsorbed nitrogen at P/P₀ = 0.995.

³V_{ultra}: volume of ultramicropores (pores < 0.7 nm).

⁴V_{micro}: volume of micropores (pores < 2.0 nm).

⁵V_{meso}: volume of mesopores (difference between V_t and V_{micro}).

Table S2. The potential differences (ΔV) between anodic and cathodic peak positions of NiS/A-PVP-NC and NiS/PI-NC.

Scan rate (mV/sec)	ΔV for NiS/A-PVP-NC (mV <i>vs.</i> SCE)	ΔV for NiS/PI-NC (mV <i>vs.</i> SCE)
10	93.2	98.3
20	116.0	129.0
40	141.5	164.3
60	163.9	192.0
80	180.3	213.4
100	197.1	227.1



© 2021 by the authors. Licensee MDPI, Basel, Switzerland. This article is an open access article distributed under the terms and conditions of the Creative Commons Attribution (CC BY) license (<http://creativecommons.org/licenses/by/4.0/>).